

Fast Calculation of Probabilistic Power Flow: A Model-based Deep Learning Approach

Yan Yang, Zhifang Yang, Juan Yu, Baosen Zhang

Abstract-- Probabilistic power flow (PPF) plays a critical role in the analysis of power systems. However, its high computational burden makes practical implementations challenging. This paper proposes a model-based deep learning approach to overcome these computational challenges. A deep neural network (DNN) is used to approximate the power flow calculation process, and is trained according to the physical power flow equations to improve its learning ability. The training process consists of several steps: 1) the branch flows are added into the objective function of the DNN as a penalty term, which improves the generalization ability of the DNN; 2) the gradients used in back propagation are simplified according to the physical characteristics of the transmission grid, which accelerates the training speed while maintaining effective guidance of the physical model; and 3) an improved initialization method for the DNN parameters is proposed to improve the convergence speed. The simulation results demonstrate the accuracy and efficiency of the proposed method in standard IEEE and utility benchmark systems.

Index Terms—Model-based deep learning, initialization methods, deep neural networks, probabilistic power flow.

I. INTRODUCTION

A. Motivation

RENEWABLE energy source generation has developed rapidly on a global scale in recent years [1], [2]. Consequently, the uncertainty in power systems has increased sharply due to the integration of these intermittent resources. This surge of uncertainty has had a significant impact on all sectors of power system operations, and makes the safe and stable operation of power grids challenging [1]. *Probabilistic power flow* (PPF) is an important fundamental tool to mitigate the impact of uncertainties through considering various random factors and providing comprehensive and important reference information for power system planning and operations [3]. Hence, there has been a recent push to integrate PPF with existing dispatch mechanism to for system with high penetration of renewables. However, while the PPF has been extensively studied in academia for decades, so far there have been few practical implementations of the PPF in power industries. The major reason for this is the heavy computational burden of the PPF method.

B. Literature Review and Background

PPF analysis methods can be generally divided into analytical methods and numerical methods. The former includes cumulant methods [4], [5], point estimation methods [6], [7], cornish-fisher expansion [8], [9] and the generalized polynomial chaos method [10]. These analytical methods is considered to be computational tractable since they directly integrate the probabilistic distribution of uncertainty factors (e.g., renewable energy source and load) into a few deterministic power flow models. However, the abovementioned methods are established based on particular assumptions that may not hold in power systems. For example, most assume the uncertainties evolve according to a Gaussian process, which is not the case for most renewable resources.

If these assumptions are not made, engineers typically use numerical methods based on Monte-Carlo simulation, which is the focus of this paper. These methods typically contain two calculation stages. First, a large number of operation statuses are sampled to reflect the probabilistic characteristics of the uncertain input factors. Then, a power flow calculation is performed for each of samples and the corresponding solutions are analyzed. Therefore, this PPF approach involves repeatedly solving an enormous number of power flow problems. Although finding the solution of individual power flow problems are not complex, it does add up when a large number of power flow calculations need to be done.

There are two ways to reduce the computational complexity in Monte-Carlo simulations. The first is to reduce the number of samples by using a smaller subset to reflect the probabilistic properties of the PPF. The representative sampling methods include importance sampling [11], Latin hypercube sampling [12], Latin supercube sampling [13] and Quasi-Monte sampling [14]. However, even the reduced sample set can still be fairly large since it has to capture complex features in uncertainties associated with renewables and load demands. There have also been proposed parallel methods to improve the efficiency of the PPF. The parallel methods can dramatically accelerate the speed using multiple GPUs [15] or cloud-computing platforms [16] without loss of accuracy. However, the hardware deployment requirement makes these methods difficult to adopt in industry.

A comparatively less studied category of methods is to speed up the computational efficiency of the power flow calculation of each sample. This approach can improve the computational efficiency of the PPF with any given number of samples, and thus it can be combined with the sampling

Y. Yang, Z. Yang, and J. Yu are with Chongqing University, Chongqing 400044, China (e-mail: cquyangyan2012@163.com, yzf1992@cqu.edu.cn, yujuan@cqu@qq.com).

B. Zhang is with the Department of Electrical and Computer Engineering, University of Washington, Seattle, WA 98195, USA (zhangbao@uw.edu).

techniques and parallel methods. One method is to use the DC power flow model in order to accelerate the nonlinear power flow calculation process. However, there are applications, especially when voltage magnitude and reactive powers are considered, where the full AC power flow model must be used [17].

The results in this paper follows the direction of using artificial neural networks to approximate and speed up the power flow calculation process [18], [19]. The PPF processes numerous samples with a similar computational task (power flow calculation), which makes it a natural target application of neural networks. To the best of our knowledge, [18] is the first paper to utilize this idea and develop a control scheme via a *radial basis function* (RBF) neural network. Followed by [19], RBF-based power flow is applied to the probabilistic PPF. However, the RBF networks are shallow models, which have difficulty extracting complex and abstract features. Besides, the RBF-based power flow calculation does not utilize the physical model of the power flow to guide the training process.

As shown by many successful examples in signal processing, *deep neural networks* (DNN) have the ability to extract more abstract and complex features compared to shallow networks (it's not difficult to show that a DNN can approximate any function with high accuracy [20], [21]). Hence, DNNs show a promising way of approximating the power flow model and tackling the computational challenge of the PPF problem. The power flow calculation of the PPF can be regarded as a nonlinear function between the system operating condition (input) and the power flow solution (output). Although the black-box characteristics of the DNN may lead to a few outliers in the power flow results, the statistical indexes of interest (e.g., mean value, standard variance and probability density function of system status) would not be affected as long as the power flow solution of the majority of samples are effectively learned. Additionally, providing sufficient data to the DNN is straightforward since both historical and synthetic samples can be used during training.

The conventional deep-learning approach is completely data-driven and does not consider the underlying physical model. In contrast, the object of interest for us (i.e., the power flow model) is completely known. Therefore, we should combine the physical models and deep-learning approaches to guide the training process. To the best of our knowledge, how this can be done has not been reported in current studies.

C. Contributions

The main contribution of this paper is to construct a DNN to approximate the power flow calculation, which significantly improves the efficiency of the PPF. The power flow model is used to improve and accelerate the learning ability of the neural network, which has the following three features:

1. A composite objective function of the DNN is proposed based on the branch flow equations. The modified DNN can more effectively extract the nonlinear complex features of the power flow model compared with a DNN trained via the

standard process.

2. The learning process is simplified to accelerate the training speed while keeping a satisfactory accuracy. Based on the physical characteristics of the transmission power grid, we remove the gradient information associated with voltage magnitudes and gradient from the phase angle to reactive powers in the learning process.

3. The rectifier linear unit and linear activation function are combined and a new initialization method is derived to improve the convergence speed.

Using the proposed method, the calculation speed of the PPF can be improved by at least 1000 times while maintaining similar accuracy as the standard iterative power flow solver.

II. BASIC STRUCTURE OF THE PROPOSED METHOD

The outline of the PPF based on a DNN is shown in Fig. 1. **Step 1** is to sample the system status. In **Step 2**, the DNN directly maps the power flow solutions of all unsolved samples without an iterative calculation. More concretely, the DNN takes in active and reactive power injections of uncertainty buses as input and outputs the complex bus voltages. It dramatically accelerate the computation speed of power flow since all operations are feed forward function evaluations. **Step 3** computes and analyzes the PPF indexes including the mean value, the standard variance and the probability density function of all the output variables.

The accuracy of the whole process is determined by the ability of the DNN to approximate the power flow model. Hence, this paper focuses on discussing how to construct the DNN for the PPF via the power flow model and the initialization method of the DNN parameters.

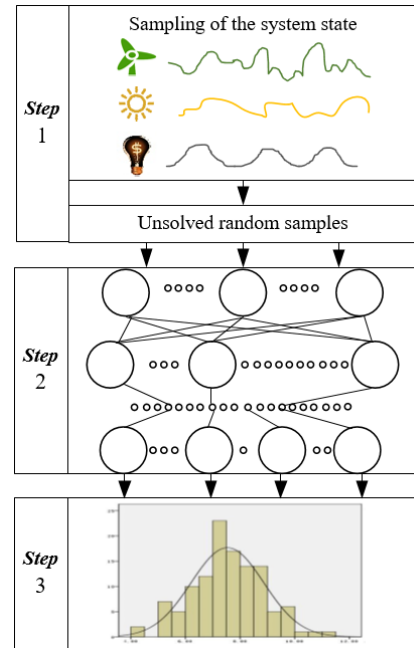


Fig. 1. Outline of PPF based on a DNN.

III. MODEL-BASED DEEP LEARNING TECHNIQUES

In this section, a modified loss function of the DNN is proposed to guide the training processing. On this basis, the

model-based deep learning process is simplified by the characteristics of the transmission grid.

A. Feature vector selection

Essentially, the DNN mines the nonlinear features/relationship of the PPF by quantifying the effect of the input changes on the output. The PPF considers the effect of bus uncertainties on power flow results, therefore the input feature vector \mathbf{X} is designed to only contain the injection power of all renewable energy sources and load demands.

The PPF requires repeatedly solving a tremendous number of deterministic power flow problems. The PPF output is concerned with bus voltages and branch flows. Therefore, the power flow problem is formulated by (1) and (2) in this paper

$$P_{ij} = G_{ij} (V_i^2 - V_i V_j \cos \theta_{ij}) - B_{ij} V_i V_j \sin \theta_{ij} \quad (1)$$

$$Q_{ij} = -B_{ij} (V_i^2 - V_i V_j \cos \theta_{ij}) - G_{ij} V_i V_j \sin \theta_{ij}, \quad (2)$$

where P_{ij} and Q_{ij} are the active and reactive branch powers from the i^{th} bus to the j^{th} bus, respectively; V_i is the voltage magnitude at bus i ; θ_{ij} is the voltage phase angle difference between bus i and bus j ; G_{ij} and B_{ij} are the conductance and susceptance between the i^{th} bus and the j^{th} bus, respectively.

Since the set of complex bus voltages (magnitude and angle) completely describes the state of the system, we set these as the output of the neural network. Other quantities of interest, for example the branch flows, can be computed once the voltages are known.

B. Loss Function Design Based on the Power Flow Equations

Essentially, training the DNN is a fitting problem. The learning target is to find the optimal DNN parameters $\theta = \{\mathbf{w}, \mathbf{b}\}$ by minimizing the loss function that describes the difference between the ideal outputs and the DNN outputs. The squared difference between the output of the NN and the label is conventionally chosen as the loss function:

$$loss = \frac{1}{m} \left\| \mathbf{Y}_{out} - \mathbf{f}_{\theta}^L(\dots \mathbf{f}_{\theta}^1(\mathbf{X}_{in})) \right\|^2. \quad (3)$$

$$\mathbf{f}_{\theta}^i(\mathbf{X}) = R_i(\mathbf{w}_i \mathbf{X} + \mathbf{b}_i) \quad (4)$$

where m is the number of training samples in each epoch; L is the number of layers; \mathbf{Y}_{out} is the normalized output vector of the PPF; \mathbf{X}_{in} is the normalized input feature vector for the PPF; R_i is the activation function at the i^{th} layer. The weight matrix \mathbf{w}_i is a $n_{i+1} \times n_i$ matrix, and the biased vector \mathbf{b}_i is a n_{i+1} -dimensional vector, where n_i is the number of neurons at the i^{th} layer.

The loss function in (3) only act on the final output value and a network trained only on it may not perform well. Therefore, we augment the loss by explicitly adding branch flow equations as penalty terms into the objective. We can do this since once the voltages are known, we can explicitly compute the branch flows, and they act as side information to further accelerate the training process. They also the training process for the accurate approximation of power flow model. The modified loss function is

$$loss_{new} = loss + \mathbf{J}(\mathbf{P}_{out}, \hat{\mathbf{P}}_{out}) + \mathbf{J}(\mathbf{Q}_{out}, \hat{\mathbf{Q}}_{out}) \quad (5)$$

where

$$\mathbf{J}(\mathbf{P}_{out}, \hat{\mathbf{P}}_{out}) = \frac{1}{m} \left\| \mathbf{P}_{out} - \hat{\mathbf{P}}_{out} \right\|^2 \quad (6)$$

$$\mathbf{J}(\mathbf{Q}_{out}, \hat{\mathbf{Q}}_{out}) = \frac{1}{m} \left\| \mathbf{Q}_{out} - \hat{\mathbf{Q}}_{out} \right\|^2, \quad (7)$$

where \mathbf{P}_{out} and \mathbf{Q}_{out} are $n_{brc} \times m$ matrices, which contain the (normalized) true branch power flows; $\hat{\mathbf{P}}_{out}$ and $\hat{\mathbf{Q}}_{out}$ are the (normalized) values computed from the output of the DNN. We normalize the flows to make each component in (5) comparable. Here we weight each component equally.

Because the learning target (i.e., the power flow model) is directly added to the objective function, the modified loss function will guide the updating process of the parameters $\theta = \{\mathbf{w}, \mathbf{b}\}$ toward an accurate approximation of the power flow calculation. To illustrate the updating process, the weight matrix \mathbf{w} is used as an example. The back-propagation process based on the RMSProp learning algorithm [22] is executed by the following equations:

$$\mathbf{w}_{(i,T+1)} = \mathbf{w}_{(i,T)} - \Delta \mathbf{w}_{(i,T)} \quad (8)$$

$$\Delta \mathbf{w}_{(i,T)} = \frac{\eta}{\sqrt{\mathbf{R}_{(i,T)} + \varepsilon}} \square d\mathbf{w}_{(i,T)} \quad (9)$$

$$\mathbf{R}_{(i,T)} = \rho * \mathbf{R}_{(i,T-1)} + (1 - \rho) * d\mathbf{w}_{(i,T)} \square d\mathbf{w}_{(i,T)} \quad (10)$$

$$d\mathbf{w}_{(i,T)} = \frac{1}{m} \sum_{k=r}^{r+m} \frac{\partial loss_{new}}{\partial \mathbf{w}_{(i,T)}} \quad (11)$$

where $\mathbf{w}_{(i,T)}$ is the weight parameters from the i^{th} layer to the $i+1^{\text{th}}$ layer at the T^{th} parameters updating; r is the sequence number of initial samples in this batch; and m is the sample size of this batch. In this paper, we use the following parameters: $\rho = 0.99$, $\eta = 0.001$, and $\varepsilon = 1 \times 10^{-8}$.

The difference of the parameter updating between the loss functions in (3) and (5) shows up in (11). From (6) and (7), we can further decompose it into

$$d\mathbf{w}_{(i,T)} = \mathbf{d}(i)^T \mathbf{y}_i / m \quad (12)$$

where

$$\mathbf{d}(i) = \mathbf{d}(i+1) \mathbf{w}_{i,T-1} \square \max(0, \mathbf{y}_i) \quad (13)$$

$$\mathbf{d}(L) = \mathbf{d}_1 + \mathbf{d}_2 + \mathbf{d}_3 \quad (14)$$

and

$$\mathbf{d}_1 = \hat{\mathbf{Y}}_{out} - \mathbf{Y}_{out} \quad (15)$$

$$\mathbf{d}_2 = \frac{(\hat{\mathbf{P}} - \mathbf{P})}{std(\mathbf{P})} \square \frac{\partial \mathbf{P}}{\partial \hat{\mathbf{Y}}_{out}} \times \frac{1}{std(\mathbf{P})} = \frac{(\hat{\mathbf{P}} - \mathbf{P})}{std(\mathbf{P})} \square \frac{\partial \mathbf{P}}{\partial \hat{\mathbf{Y}}} \times \frac{std(\mathbf{Y})}{std(\mathbf{P})} \quad (16)$$

$$\mathbf{d}_3 = \frac{(\hat{\mathbf{Q}} - \mathbf{Q})}{std(\mathbf{Q})} \square \frac{\partial \mathbf{Q}}{\partial \hat{\mathbf{Y}}_{out}} \times \frac{1}{std(\mathbf{Q})} = \frac{(\hat{\mathbf{Q}} - \mathbf{Q})}{std(\mathbf{Q})} \square \frac{\partial \mathbf{Q}}{\partial \hat{\mathbf{Y}}} \times \frac{std(\mathbf{Y})}{std(\mathbf{Q})} \quad (17)$$

In equations (16) and (17), \mathbf{Y} is the output vector of the PPF; $\hat{\mathbf{Y}}_{out}$ is the (normalized) output of the DNN; $\hat{\mathbf{Y}}$ is the anti-normalized value of $\hat{\mathbf{Y}}_{out}$; and \square is a Hadamard multiplier.

From (12)-(14), we can see that $\mathbf{d}(L)$ will directly affect the updating direction of the weight parameters \mathbf{w} . The modified loss function guides the updating of the DNN parameters by modifying $\mathbf{d}(L)$. The following focuses on the impact of the modified function on the value of $\mathbf{d}(L)$ in detail.

Using the conventional loss function (3), $\mathbf{d}(L)$ only contains \mathbf{d}_1 . The added plenty terms (6) (7) affect $\mathbf{d}(L)$ via \mathbf{d}_2 and \mathbf{d}_3 , respectively. From (8)-(17), the modified loss function in (5) increases the updating step size of the weight parameters \mathbf{w} when the updating direction simultaneous reduces (3), (6) and (7). Meanwhile, the proposed loss function is expected to reduce/prevent DNN over fitting the bus voltage when the parameter updating directions for (3), (6) and (7) are different. Numerical studies in Section V demonstrate how the proposed method can promote the training convergence.

We can also control the contribution of \mathbf{d}_2 and \mathbf{d}_3 to the output feature vector ($\mathbf{Y}_{out} = [\mathbf{V}, \boldsymbol{\theta}]$). The output feature contains the voltage magnitude and voltage phase angle. Therefore, two contribution weights α and β for updating the voltage magnitude and the phase angle are respectively proposed, which are shown in (18).

$$\begin{aligned} \mathbf{d}_V[L] &= \mathbf{d}_{1,V} + \alpha(\mathbf{d}_{2,V} + \mathbf{d}_{3,V}) \\ \mathbf{d}_\theta[L] &= \mathbf{d}_{1,\theta} + \beta(\mathbf{d}_{2,\theta} + \mathbf{d}_{3,\theta}) \\ \mathbf{d}[L] &= [\mathbf{d}_V[L], \mathbf{d}_\theta[L]] \end{aligned} \quad (18)$$

where $\mathbf{d}_V[L]$, $\mathbf{d}_{1,V}$, $\mathbf{d}_{2,V}$, and $\mathbf{d}_{3,V}$ are a part of vector $\mathbf{d}[L]$, \mathbf{d}_1 , \mathbf{d}_2 , and \mathbf{d}_3 , respectively, where the DNN output is only the voltage magnitude (similarly for the $\mathbf{d}_\theta[L]$, $\mathbf{d}_{1,\theta}$, $\mathbf{d}_{2,\theta}$, and $\mathbf{d}_{3,\theta}$).

This strategy is amount to a form of regularization in the deep learning. The contribution of $\mathbf{d}_2+\mathbf{d}_3$ to the output feature vector should not be much larger than that of \mathbf{d}_1 . An empirical formula (19) is designed to determine the values of α and β .

$$\begin{aligned} \alpha &= 0.5 \times \frac{\max(\text{abs}(\mathbf{d}_{1,V}))}{\max(\text{abs}(\mathbf{d}_{2,V} + \mathbf{d}_{3,V}))} \\ \beta &= 0.5 \times \frac{\max(\text{abs}(\mathbf{d}_{1,\theta}))}{\max(\text{abs}(\mathbf{d}_{2,\theta} + \mathbf{d}_{3,\theta}))} \end{aligned} \quad (19)$$

where \max is a function that returns the maximum value, and abs is a function that returns the absolute value.

C. Model-based Simplification of Learning Process

The modified loss function can guide the training process and reduce the number of epochs. However, it does add more steps within each epoch. Here we use the characteristics of the transmission grid to again simplify the training process.

By standard calculation, the power flow sensitivities are:

$$\frac{\partial P_{ij}}{\partial \theta_i} = G_{ij}V_iV_j \sin \theta_{ij} - B_{ij}V_iV_j \cos \theta_{ij} = -\frac{\partial P_{ij}}{\partial \theta_j} \quad (20)$$

$$\frac{\partial Q_{ij}}{\partial \theta_i} = -B_{ij}V_iV_j \sin \theta_{ij} - G_{ij}V_iV_j \cos \theta_{ij} = -\frac{\partial Q_{ij}}{\partial \theta_j} \quad (21)$$

$$\frac{\partial P_{ij}}{\partial V_i} = 2G_{ij}V_j - V_j(G_{ij} \cos \theta_{ij} + B_{ij} \sin \theta_{ij}) \quad (22)$$

$$\frac{\partial P_{ij}}{\partial V_j} = V_i(G_{ij} \cos \theta_{ij} + B_{ij} \sin \theta_{ij}) \quad (23)$$

$$\frac{\partial Q_{ij}}{\partial V_i} = -2B_{ij}V_j + V_j(B_{ij} \cos \theta_{ij} - G_{ij} \sin \theta_{ij}) \quad (24)$$

$$\frac{\partial Q_{ij}}{\partial V_j} = V_i(B_{ij} \cos \theta_{ij} - G_{ij} \sin \theta_{ij}) \quad (25)$$

The training process with the modified loss function can be activated by directly feeding equations (20)-(25) into (16) and (17). We find some parts of (20)-(25) have very little impact on the training process. Therefore, we can reduce the computational complexity through two simple steps.

i) Removing the impact of voltage magnitude

As mentioned above, the DNN mines the nonlinear features/relationship of the PPF by quantifying the effect of the input changes on the output. In power systems, the voltage magnitude normally only fluctuates within $\pm 5\%$ per unit. However, the change range of the bus phase angle can reach more than 30° with the operation condition. Therefore, the impact of the model guidance on the voltage magnitude is much smaller than that of the phase angle.

From the perspective of computational complexity, including the voltage magnitude incurs more computational cost than phase voltage. According to (14)-(17), the voltage magnitude term shows up in all of (20)-(25). Therefore, the computational cost of including the sensitivity of voltage magnitude is approximately twice that of the angle phase. Hence we remove the sensitivity terms associated with the voltage magnitude in the training process.

ii) Removing the reactive guidance for the phase angle

We further focus on the sensitivity of the phase angle according to formulas (20) and (21). In the transmission grid, we can generally have:

$$\begin{aligned} |B_{ij}| \square |G_{ij}|, \\ B_{ij} > 0, G_{ij} < 0, \text{ and } i \neq j \end{aligned} \quad (26)$$

Although the bus phase angle can change sharply with the operation condition, the phase angle difference of the two buses remains a relatively small number. Thus, we can have:

$$\sin \theta_{ij} < \cos \theta_{ij} \quad (27)$$

According to formulas (26) and (27), it can be easily derived that the absolute value of formula (21) is much less than formula (20). Additionally, the absolute value of $(\hat{\mathbf{Q}}-\mathbf{Q})$ is generally less than that of $(\hat{\mathbf{P}}-\mathbf{P})$, because the voltage magnitude is easier to learn than phase angle. The absolute value of $\text{std}(\mathbf{P})$ is generally less than that of $\text{std}(\mathbf{Q})$, because the active load demand is higher than the reactive load demand in practice. Therefore, it can be concluded from (12)-(17) that the reactive branch power has a much lower impact on the training process compared to the active power flow. In consequence, we ignore the impact of reactive power on the phase angles.

In summary, the training process is simplified as follows.

$$(8)-(10) \quad (28)$$

$$(12)-(13) \quad (29)$$

$$\mathbf{d}(L) = \mathbf{d}_1 + \mathbf{d}_{1,\theta} \quad (30)$$

$$\mathbf{d}_1 = \hat{\mathbf{Y}}_{out} - \mathbf{Y}_{out} \quad (31)$$

$$\mathbf{d}_{1,\theta} = \mathbf{d}_{1,\theta} + \alpha \frac{(\hat{\mathbf{P}} - \mathbf{P})}{std(\mathbf{P})} \square \frac{\partial \mathbf{P}}{\partial \boldsymbol{\theta}} \times \frac{std(\boldsymbol{\theta})}{std(\mathbf{P})}. \quad (32)$$

It's interesting to note that both approximations, assuming voltage magnitudes are roughly constant and ignoring the impact of reactive power on angles, are standard and often made in power flow analysis problems. So it is not surprising that they are also helpful in the training of DNN.

IV. ACTIVATION FUNCTION AND INITIALIZATION METHOD

A. Designed Activation Function

The activation function has a crucial impact on the training process. *Rectifier linear unit* (ReLU) activation functions are easier to train compared to traditional sigmoid-like activation functions, which has been reported in [23]. Additionally, a theoretical initialization method considering the ReLU function was derived in [24]. Therefore, we select ReLU as the activation function:

$$R_i(x) = \begin{cases} x & \text{if } x > 0 \\ 0 & \text{if } x \leq 0 \end{cases} \quad (33)$$

To improve the training efficiency of DNN, the input and output data of the PPF should be preprocessed to eliminate the adverse influence of outlier samples and the numerical problem in the training process. The z-score method shown in (34) is adopted to normalize the samples. This method can effectively handle outliers, and the mean and standard variance of the historical statistics are only required. Moreover, it can reserve the distribution characteristics more effectively than other preprocessing methods such as min-max method.

$$\mathbf{v}_{out} = \begin{cases} \frac{\mathbf{v} - v_{mean}}{v_{std}} & \text{if } v_{std} \neq 0 \\ \mathbf{v} - v_{mean} & \text{if } v_{std} = 0 \end{cases} \quad (34)$$

where v_{mean} and v_{std} are the mean and the standard deviation of vector \mathbf{v} , respectively.

The normalized output can be less than zero, but the ReLU cannot reach a value less than zero. Therefore, the activation function of the last layer is designed to be linear as in (35). This idea has also been reported in many version problems to give a wide range for the output [25].

$$R_L(x) = x \quad (35)$$

B. Corresponding Initialization Method

The DNN parameters initialization can directly affect the training efficiency and even the convergence. In recent years, some studies have been reported, which can be categorized into two types: adding a pretraining stage to initialize the DNN [26], and random initialization approaches [24], [27]-[28]. The former one requires more training time and may also lead to a poor local optimum. Therefore, this paper focus on the latter. The latest random initialization method that particularly considers ReLU is proposed in [24].

In this paper, the ReLU and linear activation functions are combined. Hence, a new initialization approach is derived to improve the PPF learning efficiency. We define \mathbf{y}_i and \mathbf{z}_i as the

activation vector and the argument vector at the i^{th} layer.

i) Forward propagation case

We then have:

$$\mathbf{z}_i = \mathbf{w}_i \mathbf{y}_i + \mathbf{b}_i, \quad \mathbf{y}_i = R_i(\mathbf{z}_{i-1}) \quad (36)$$

Considering the hypothesis that the elements of \mathbf{y}_i and \mathbf{z}_i are mutually independent, as well as \mathbf{y}_i and \mathbf{z}_i are independent of each other [24][27]. We then have:

$$Var[\mathbf{z}_i] = n_i Var[\mathbf{w}_i \mathbf{y}_i] \quad (37)$$

where \mathbf{y}_i , \mathbf{z}_i , and \mathbf{w}_i denote to the random variables of each element in \mathbf{y}_i , \mathbf{z}_i and \mathbf{w}_i . We can obtain:

$$Var[\mathbf{z}_i] = n_i Var[\mathbf{w}_i] E(\mathbf{y}_i^2) \quad (38)$$

As in [24] and [27], let w_{i-1} has a symmetric distribution around zero and $b_{i-1}=0$. Then, z_{i-1} has a zero mean and has a symmetric distribution. Because y_i is obtained by the ReLU function, we can have $E[y_i^2] = \frac{1}{2} E[z_{i-1}^2] = \frac{1}{2} Var[z_{i-1}]$. Then,

$$Var[\mathbf{z}_i] = \frac{1}{2} n_i Var[\mathbf{w}_i] Var[\mathbf{z}_{i-1}] \quad (39)$$

Similarly, we have:

$$Var[\mathbf{z}_{L-1}] = Var[\mathbf{z}_1] \left(\prod_{i=2}^{L-1} \left(\frac{1}{2} n_i Var[\mathbf{w}_i] \right) \right) \quad (40)$$

This equation is the key to the initialization design. A proper initialization method should avoid reducing or magnifying the magnitudes of input signals exponentially. Therefore, a sufficient condition is:

$$\frac{1}{2} n_i Var[\mathbf{w}_i] = 1, \quad i \geq 2 \quad (41)$$

When $i=1$, we have $z_1 = w_1 y_0$, where y_0 represents the input signal. Because there is no ReLU applied on the input signal, we have

$$Var[\mathbf{w}_1] = \frac{1}{n_1} \quad (42)$$

In conclusion,

$$Var[\mathbf{w}_i] = \begin{cases} \frac{2}{n_i} & i \neq 1 \\ \frac{1}{n_i} & i = 1 \end{cases}, \quad i = 1, \dots, L-1 \quad (43)$$

ii) Backward propagation case

For the back-propagation process, we obtain the following:

$$\frac{\partial loss}{\partial \mathbf{y}_{i-1}} = \mathbf{w}_i^T \frac{\partial loss}{\partial \mathbf{z}_i}, \quad \frac{\partial loss}{\partial \mathbf{z}_i} = R_i'(\mathbf{z}_i) \frac{\partial loss}{\partial \mathbf{y}_i} \quad (44)$$

where T is a transfer function; and \mathbf{w}_i^T can be obtained by transposing the elements of \mathbf{w}_i .

Similar to the forward propagation case, we assume that w_i and $\partial loss / \partial z_i$ are independent of each other. We then have:

$$Var \left[\frac{\partial loss}{\partial \mathbf{y}_{i-1}} \right] = n_{i+1} Var[\mathbf{w}_i] E \left[\left(\frac{\partial loss}{\partial \mathbf{z}_i} \right)^2 \right] \quad (45)$$

Additionally, $\partial loss / \partial \mathbf{y}_{i-1}$ has a zero mean for all layers when w_i is initialized by a symmetric distribution around zero.

We assume that R' and $\partial loss/\partial y_i$ are independent of each other. Because all but the last activation function are ReLU, we have:

$$E \left[\left(\frac{\partial loss}{\partial z_i} \right)^2 \right] = \begin{cases} E \left[\left(\frac{\partial loss}{\partial y_i} \right)^2 \right] = Var \left[\frac{\partial loss}{\partial y_i} \right] & i = L-1 \\ \frac{1}{2} E \left[\left(\frac{\partial loss}{\partial y_i} \right)^2 \right] = \frac{1}{2} Var \left[\frac{\partial loss}{\partial y_i} \right] & i \neq L-1 \end{cases} \quad (46)$$

If we consider a sufficient condition that the gradient is not exponentially large/small, we can then have:

$$Var[w_i] = \begin{cases} 1/n_{i+1} & i = L-1 \\ 2/n_{i+1} & i \neq L-1, i = 1, \dots, L-1 \end{cases} \quad (47)$$

As a compromise between formulas (43) and (47), we might want to have:

$$Var[w_i] = \begin{cases} \frac{n_i + 2n_{i+1}}{n_i n_{i+1}} & i = L-1 \\ \frac{n_i + n_{i+1}}{n_i n_{i+1}} & i = 2, \dots, L-2 \\ \frac{2n_i + n_{i+1}}{n_i n_{i+1}} & i = 1 \end{cases} \quad (48)$$

Consequently, the DNN weight parameter w is initialized in a zero-mean Gaussian distribution whose standard variance is shown in (49), and \mathbf{b} is initialized as 0.

$$Std[w_i] = \begin{cases} \sqrt{\frac{n_i + 2n_{i+1}}{n_i n_{i+1}}} & i = L-1 \\ \sqrt{\frac{n_i + n_{i+1}}{n_i n_{i+1}}} & i = 2, \dots, L-2 \\ \sqrt{\frac{2n_i + n_{i+1}}{n_i n_{i+1}}} & i = 1 \end{cases} \quad (49)$$

From formulas (43), (47) and (48), we can observe that the initialization of the middle-layer weight parameters \mathbf{w} can meet both cases when the amounts of middle-layer neurons are equal. Therefore, we set the number of hidden neurons in each layer to be the same in our experiments.

V. SIMULATION TESTS

The effectiveness of the proposed methods is verified in a modified IEEE 30-bus system, an IEEE 118-bus system and a practical 661-bus utility system.

A. Test Information and Methods for Comparison

The penetration of renewable energy sources reaches 30% in both the modified IEEE 30-bus and the 118-bus systems. The random characteristics of wind farms and photovoltaic stations can be found in [29]. The load demand is sampled randomly via a normal distribution with a standard deviation (10% of the expected values).

Monte-Carlo simulation method based on Newton-Raphson algorithm is the PPF benchmark. Following six methods are compared to verify the effectiveness of the proposed methods.

M1: A DNN where the parameters are randomly initialized by reference [24].

M2: A DNN with the modified loss function.

M3: A DNN with the proposed initialization method.

M4: A DNN with the proposed initialization method and the modified loss function.

M5: A DNN that is the same with M4, but the guidance of the voltage magnitude is removed.

M6: A DNN that is the same with M5, but the reactive guidance of the phase angle is removed.

These comparison methods and the corresponding intentions are listed in the Table I.

TABLE I COMPARISON METHODS AND THE INTENTION

Methods	Corresponding intention
M1 and M2	Verify the effectiveness of the proposed loss function
M1 and M3	Verify the effectiveness of the proposed initialization method
M1, M2, M3 and M4	Verify the effectiveness of the combination of the initialization and basic model-based approaches.
M1 M4, and M5	Verify the effectiveness of removing the guidance of the voltage magnitude
M1, M4, M5, and M6	Verify the effectiveness of the combination of the initialization and simple model-based approaches.

Above methods have the same hyper parameters for each case, which are given in Table II. The number of validation samples and test samples are both 10000. The training process is stopped if the DNN meets the condition of the early stop method [30] or the number of epochs reaches the threshold.

TABLE II HYPER PARAMETERS FOR DIFFERENT CASES

Cases	Hidden layers	The number of training data
Case 30	[100 100 100]	10000
Case 118	[200 200 200]	20000
Case 661	[500 500 500 500 500]	70000

To compare the performances of the different methods, some indexes are proposed. N_{epoch} refers to the number of epochs. V_{loss} means the value of the original loss function (3). P_{vm} refers to the proportion of the absolute error of the voltage magnitude that exceeds 0.0001 p.u. P_{va} refers to the proportion of the absolute error of the phase exceeds 0.01 rad. P_{pf} / P_{qf} refers to the proportion of the absolute error of the active / reactive branch power that exceeds 5 MW.

B. Validation of the Initialization Method and Modified Loss Function

TABLE III PERFORMANCE COMPARISONS AMONG M1, M2, AND M3 FOR DIFFERENT CASES

Cases	Method	N_{epoch}	V_{loss}	P_{vm}	P_{va}	P_{pf}	P_{qf}
Case 30	M3	1000	1157	6.7%	0.0%	0.0%	0.0%
	M2	1000	1175	4.0%	0.0%	0.0%	0.0%
	M1	1000	1175	6.3%	0.0%	0.0%	0.0%
Case 118	M3	1000	44	2.7%	0.0%	3.5%	0.0%
	M2	1000	75	4.7%	0.1%	7.6%	0.3%
	M1	1000	80	5.4%	0.0%	8.1%	0.4%
Case 661	M3	500	3984	3.6%	0.0%	3.9%	0.0%
	M2	500	4185	4.3%	0.0%	3.7%	0.0%
	M1	500	4269	4.4%	0.0%	6.2%	0.0%

Table III shows the performance comparisons among M1, M2 and M3 with the same number of epochs for different cases. It can be observed from Table III that the proposed loss function M2 can reduce the value of the original loss function and obtain a better generality ability in Case 118 and Case 661. In Case 30, although the value of the loss function is not

reduced by M3, the generality ability still has an obvious improvement. Therefore, the proposed modified loss function method can guide the training process effectively.

It can also be observed from Table III that the proposed improved initialization method M3 can reduce V_{loss} faster and obtain a better generality ability compared to the initialization method M1 in [24]. Specifically, the value of V_{loss} can almost be cut in half by the proposed initialization method M2 in Case 118. Therefore, the derived initialization method can improve the convergence efficiency effectively.

When the number of epochs is fixed, it can be seen from Table IV that the proposed method M4 can make all the accuracy indexes meet the accuracy requirements ($\leq 5\%$), while one or two indexes cannot achieve the requirements using method M1 (marked in bold). Additionally, comparing the results of Table IV and III, it can be concluded that the combination can achieve better results than the individual proposed method.

TABLE IV PERFORMANCE COMPARISON BETWEEN M1 AND M4 UNDER THE SAME EPOCHS FOR EACH CASE

Cases	Method	N_{epoch}	V_{loss}	P_{vm}	P_{va}	P_{pf}	P_{af}
Case 30	M4	1000	1175	3.6%	0.0%	0.0%	0.0%
	M1	1000	1175	6.3%	0.0%	0.0%	0.0%
Case 118	M4	1000	41	2.8%	0.1%	3.2%	0.0%
	M1	1000	80	5.4%	0.0%	8.1%	0.4%
Case 661	M4	500	3877	3.9%	0.0%	3.4%	0.0%
	M1	500	4269	4.4%	0.0%	6.2%	0.0%

TABLE V PERFORMANCE COMPARISON BETWEEN M1 AND M4 WHEN MEETING THE ACCURACY REQUIREMENTS

Cases	Method	N_{epoch}	V_{loss}	P_{vm}	P_{va}	P_{pf}	P_{af}
Case 30	M4	507	1205	$\leq 5\%$	$\leq 5\%$	$\leq 5\%$	$\leq 5\%$
	M1	1620	1146	$\leq 5\%$	$\leq 5\%$	$\leq 5\%$	$\leq 5\%$
Case 118	M4	569	64	$\leq 5\%$	$\leq 5\%$	$\leq 5\%$	$\leq 5\%$
	M1	2012	41	$\leq 5\%$	$\leq 5\%$	$\leq 5\%$	$\leq 5\%$
Case 661	M4	145	4871	$\leq 5\%$	$\leq 5\%$	$\leq 5\%$	$\leq 5\%$
	M1	375	4521	$\leq 5\%$	$\leq 5\%$	$\leq 5\%$	$\leq 5\%$

The training process is stopped as soon as all the indexes by DNN being no more than 5%, with the results shown in Table V. It can be observed that N_{epoch} of M1 can be reduced by 68.7%, 71.7% and 61.3% by the proposed method M4 in the three cases, respectively. Additionally, it is worth noting that the value of P_{pf} by M1 increases with the number of epochs between Tables III and V for case 661. This phenomenon is called ‘‘over fitting’’. Without the guidance of the physical model and a suitable initial value, the branch flow accuracy cannot be guaranteed, even though the values of most bus voltages are approximated quite well. Moreover, the value of P_{pf} calculated by M4 is 1.6%. However, it is almost impossible to achieve an improvement of 1.6% using M1.

Above all, the proposed loss function and initialization method can speed up the convergence dramatically and can reduce or prevent the DNN over fitting the bus voltage.

C. Validation of the Model-based simplification

i) Performance comparison

Table VI shows the performance comparison among M1, M5, and M6. It can be observed that method M5 still has a significant advantage over M1. Comparing Table VI with Table V, it can be observed the number of epochs to meet the accuracy requirements using M5 is less than that of M4 in Case 118 and Case 661 (expressed by arrows). In Case 30, the

number of epochs rise from 507 to 576, but it is tolerable in the small-scale case. Therefore, the simplification that removing the guidance of the voltage magnitude in the learning process can also maintain an excellent performance, and even have a better one.

The reactive guidance of the phase angle is further removed, and the numerical simulation of M6 is shown in Table VI. It can be observed that the decreasing or increasing trend of N_{epoch} for M6 is the same as M5 compared to M4. In Case 661, N_{epoch} of M8 is further reduced compared to M5, and N_{epoch} of M1 can be reduced by 74.1%.

In conclusion, the removals of the guidance for the voltage magnitude and the reactive guidance for the phase angle are reasonable, which can lead to equally matched results, or even better ones.

TABLE VI PERFORMANCE COMPARISON AMONG M1, M5 AND M6 WHEN MEETING THE ACCURACY REQUIREMENTS

Cases	Method	N_{epoch}	V_{loss}	P_{vm}	P_{va}	P_{pf}	P_{af}
Case 30	M6	775 \uparrow	1200	$\leq 5\%$	$\leq 5\%$	$\leq 5\%$	$\leq 5\%$
	M5	576 \uparrow	1195	$\leq 5\%$	$\leq 5\%$	$\leq 5\%$	$\leq 5\%$
	M1	1620	1146	$\leq 5\%$	$\leq 5\%$	$\leq 5\%$	$\leq 5\%$
Case 118	M6	622 \downarrow	62	$\leq 5\%$	$\leq 5\%$	$\leq 5\%$	$\leq 5\%$
	M5	552 \downarrow	67	$\leq 5\%$	$\leq 5\%$	$\leq 5\%$	$\leq 5\%$
	M1	2012	41	$\leq 5\%$	$\leq 5\%$	$\leq 5\%$	$\leq 5\%$
Case 661	M6	97 \downarrow	4887	$\leq 5\%$	$\leq 5\%$	$\leq 5\%$	$\leq 5\%$
	M5	106 \downarrow	4887	$\leq 5\%$	$\leq 5\%$	$\leq 5\%$	$\leq 5\%$
	M1	375	4521	$\leq 5\%$	$\leq 5\%$	$\leq 5\%$	$\leq 5\%$

ii) Computation time comparison

Table VII shows the computation time of each epoch with the different methods. As expected, the simplified methods M5 and M6 cost less time than the basic model-based deep learning method M4 in all cases. In Case 30 and Case 118, the computation time with different methods does not have a significant difference. However, for a large practical power system, the difference is significantly obvious.

With the removal of the guidance for the voltage magnitude, method M5 can reduce the computation time by 6.64 seconds for each epoch compared to M4. The computation time using M4 can be further reduced by 8.35 seconds by removing the reactive guidance for phase angle M6. The speed advantage of the simplified model-based deep learning method will increase with the number of epochs.

Above all, the proposed simplified model-based deep learning method M6 can reduce the computational pressure significantly compared to the basic model-based deep learning method M4, while maintaining a comparable performance.

TABLE VII COMPUTATION TIME COMPARISON OF EACH EPOCH WITH DIFFERENT METHODS

Cases	$t_{M1}(s)$	$t_{M4}(s)$	$t_{M5}(s)$	$t_{M6}(s)$
Case 30	0.13	0.26	0.21	0.20
Case 118	0.68	1.64	1.25	1.09
Case 661	35.21	51.53	45.07	43.18

D. Performance of the Proposed Method for the PPF

The above numerical experiments have demonstrated the accuracy performance of the proposed method for calculating the PPF. The computation time comparison between the DNN and the benchmark PPF is shown in Table VIII. It can be seen that the proposed DNN method can accelerate the calculation speed by 1234 to 2040 times compared to the benchmark PPF. Therefore, the proposed approach provides an opportunity for the online application of PPF.

TABLE VIII COMPUTATION TIME COMPARISON BETWEEN DNN AND THE PPF BENCHMARK WITH 10000 TEST SAMPLES

Cases	Trained DNN (s)	Benchmark (s)	Acceleration ratio
Case 30	0.04	81.59	2040
Case 118	0.13	208.02	1600
Case 661	0.82	1012.19	1234

VI. CONCLUSION

This paper proposes a model-based deep learning approach to quickly calculate the solution to power flow equations, with the main application in speeding up probabilistic power flow calculations. Based on the branch flow equations, a composite loss function is proposed to guide the training process. Combined with the physical characteristics of the transmission grid, the model-based training process method is simplified by removing the impact of voltage magnitudes and the dependence between reactive power and angles. The proposed simplified method can accelerate the training speed while maintaining a comparable performance. In addition, an improved initialization method for the deep neural network parameters is derived to further improve the convergence efficiency. Simulation results using IEEE test benchmarks demonstrate the effectiveness of the individually proposed methods against standard power flow solvers and other learning-based methods. We show the calculation speed of power flow problems can be accelerated by three orders of magnitude, thus allowing operators to consider 1000 times more samples under the same time constraints.

REFERENCES

- [1] Y. Wang, N. Zhang, C. Kang, M. Miao, R. Shi, and Q. Xia, "An efficient approach to power system uncertainty analysis with high-dimensional dependencies," *IEEE Trans. Power Syst.*, vol. 33, pp. 2984-2994, 2017.
- [2] Y. Yang, J. Yu, M. Yang, P. Ren, Z. Yang, G. Wang, "Probabilistic modeling of renewable energy source based on spark platform with large-scale sample data," *Int. Trans. Electr. Energ. Syst.*, vol. 29, no.3, pp: 1-13, 2019.
- [3] S. Gottwalt, J. Gärtner, H. Schmeck and C. Weinhardt, "Modeling and valuation of residential demand flexibility for renewable energy integration," in *IEEE Trans. Smart Grid*, vol. 8, no. 6, pp. 2565-2574, Nov. 2017.
- [4] F. Miao, V. Vittal, G. T. Heydt, R. Ayyanar, "Probabilistic power flow studies for transmission systems with photovoltaic generation using cumulants," *IEEE Trans. Power Syst.*, vol. 27, no.4, pp.2251-2261, 2012.
- [5] W. Wu, K. Wang, G. Li, X. Jiang and Z. Wang, "Probabilistic load flow calculation using cumulants and multiple integrals," *IET Generation, Transmission & Distribution*, vol. 10, no. 7, pp. 1703-1709, May 2016.
- [6] P. Caramia, G. Carpinelli, and P. Varilone, "Point estimate schemes for probabilistic three-phase load flow," *Elect. Power Syst. Res.*, vol.80, no. 2, pp.168-175, 2010.
- [7] C.-L. Su, "Probabilistic load-flow computation using point estimate method," *IEEE Trans. Power Syst.*, vol. 20, no. 4, pp. 1843-1851, Nov. 2005.
- [8] F. J. Ruiz-Rodriguez, J. C. Hernandez, F. Jurado, "Probabilistic load flow for photovoltaic distributed generation using the Cornish-Fisher expansion," *Elect. Power Syst. Res.*, vol. 89, pp. 129-138, 2012.
- [9] J. Usaola, "probabilistic load flow with wind production uncertainty using cumulants and Cornish-Fisher expansion," *Int. J. Elec. Power and Energ. Syst.*, vol. 31, no. 9, pp. 474-481, 2009.
- [10] H. Wu, Y. Zhou, S. Dong, Y. Song, "Probabilistic load flow based on generalized polynomial chaos," *IEEE Trans. Power Syst.*, vol. 32, no.1, Jan. 2017.
- [11] P. Wang, J. Zhang, Q. Gong, C. Tan, Y. Zhu and Y. Fan, "Reliability analysis of Bayesian Monte Carlo adaptive importance sampling method for structural safety," *Proc. 9th Int. Conf. Rel., Maintainability and Safety*, Guiyang, 2011, pp. 440-444.
- [12] H. Yu, C. Y. Chung, K. P. Wong, H. W. Lee, J. H. Zhang, J. H. Zhang, "Probabilistic load flow evaluation with hybrid Latin hypercube sampling and Cholesky decomposition," *IEEE Trans. Power Syst.*, vol. 24, no. 2, pp. 661-667, 2009.
- [13] M. Hajian, W. D. Rosehart, H. Zareipour, "Probabilistic power flow by monte carlo simulation with latin supercube sampling," *IEEE Trans. Power Syst.*, vol. 28, no. 2, pp. 1550-1559, May 2013.
- [14] Z. Q. Xie, T. Y. Ji, M. S. Li and Q. H. Wu, "Quasi-Monte Carlo Based probabilistic optimal power flow considering the correlation of wind speeds using Copula function," *IEEE Trans. Power Syst.*, vol.33, no.2, pp. 2239-2247, Aug. 2017.
- [15] G. Zhou, R. Bo, L. Chien, X. Zhang, S. Yang and D. Su, "GPU-accelerated algorithm for online probabilistic power flow," *IEEE Trans. Power Syst.*, vol. 33, no. 1, pp. 1132-1135, Jan. 2018.
- [16] D. Wang, F. Zhou, J. Li, "Cloud-based parallel power flow calculation using resilient distributed datasets and directed acyclic graph," *J. Mod. Power Syst. Clean Energ.*, vol. 7, no. 1, pp. 65-77, Jan. 2019.
- [17] G. Mokhtaei, A. Rahiminezhad, A. Behnood, J. Ebrahimi, G. B. Gharehpetian, "Probabilistic DC load-flow based on two-point estimation method," *4th Int. Power Eng. and Optimization Conf.*, Shah Alam, Selangor, 2010, pp. 287-291.
- [18] H. R. Baghaee, M. Mirsalim, G. B. Gharehpetian, "Power calculation using RBF neural networks to improve power sharing of hierarchical control scheme in multi-DER microgrids," *IEEE J. Emerg. Sel. Top. Power Electron.*, vol. 4, no. 4, pp. 1217-1225, 2016.
- [19] H. R. Baghaee, M. Mirsalim, G. B. Gharehpetian and H. A. Talebi, "Fuzzy unscented transform for uncertainty quantification of correlated wind/PV microgrids: possibilistic-probabilistic power flow based on RBFNNs," *IET Renewable Power Generation*, vol. 11, no. 6, pp. 867-877, May 2017.
- [20] M. Leshno, V. Y. Lin, A. Pinkus, and S. Schocken, "Multilayer feedforward networks with a nonpolynomial activation function can approximate any function," *Neural Networks*, vol. 6, pp. 861-867, 1993.
- [21] U. Shaham, A. Cloninger, R.R. Ronald, "Provable approximation properties for deep neural networks," *Appl. & Comput. Harmonic Anal.*, vol. 44, no. 3, pp. 537-557, May 2018.
- [22] H. Zulkifli, Understanding Learning Rates and How It Improves Performance in Deep Learning. [Online]. Available: <https://towardsdatascience.com/understanding-learning-rates-and-how-it-improves-performance-in-deep-learning-d0d4059c1c10>.
- [23] Glorot X, Bordes A, Bengio Y, "Deep sparse rectifier neural networks," *Proce. 14th Int. Conf. Artificial Intell. and Statist.*, Fort Lauderdale, USA, 2011, pp. 315-323.
- [24] K. He, X. Zhang, S. Ren and J. Sun, "Delving deep into Rectifiers: surpassing human-level performance on ImageNet classification," *IEEE Int. Conf. Comput. Vision*, Santiago, USA, 2015, pp. 1026-1034.
- [25] D. Eigen, C. Puhrsch, R. Fergus. Depth map prediction from a single image using a multi-scale deep network. 2014. Available: arXiv:1406.2283.
- [26] K. Simonyan and A. Zisserman. Very deep convolutional networks for large-scale image recognition. 2014. Available: arXiv:1409.1556.
- [27] X. Glorot and Y. Bengio, "Understanding the difficulty of training deep feed forward neural networks," *Int. Conf. on Artificial Intell. and Statist.*, 2010, pp. 249-256.
- [28] A. Krizhevsky, I. Sutskever, and G. Hinton, "Imagenet classification with deep convolutional neural networks," *Proc. 25th Int. Conf. Neural Inform. Proc. Syst.*, Nevada, USA, Dec. 2012, pp. 1097-1105.
- [29] Z. Qin, W. Li, X. Xiong, "Incorporating multiple correlations among wind speeds, photovoltaic powers and bus loads in composite system reliability evaluation," *Appl. Energ.*, vol. 110, no. 5, pp. 285-294, Oct. 2013.
- [30] G. Raskutti, M. J. Wainwright, B. Yu, "Early stopping for non-parametric regression: an optimal data-dependent stopping rule," *J. Mach. Learning Res.*, vol. 15, no. 1, pp. 1318-1325, 2014.